修 士 論 文 の 和 文 要 旨

研究科・専攻	大学院　情報理工学研究科　情報・ネットワーク工学専攻　博士前期課程		
氏　　名	追永　大	学籍番号	1831024
論 文 題 目	逐次干渉除去と ZigZag 復号に基づく ランダムアクセスプロトコルの解析と設計		

要 旨

超多数の端末が散発的に通信するネットワークの実現のため，多元接続方式としてランダムアクセスを適用する研究が多くなされている．ランダムアクセスの一種である非正則繰り返しスロット化 ALOHA(IRSA: Irregular Repetition Slotted ALOHA) は，パケット復調の手段として逐次干渉除去を用いて高いスループット性能を達成するものの，高負荷時における性能の劣化が著しいことが知られている．そこで，本研究では逐次干渉除去に加えてジグザグ復号を組み合わせることで高負荷時におけるスループット性能の劣化を抑圧するジグザグ復号可能な符号化スロット化 ALOHA(ZDCSA: Zigzag Decodable Coded Slotted ALOHA) および拡張 ZDCSA(EZDCSA: Enhanced-ZDCSA) を提案する．一方で，IRSA と異なり時間フレーム長が固定でないフレームレス ALOHA が提案されており，逐次干渉除去に加えてキャプチャ効果を適用した場合の性能解析がなされている．キャプチャ効果を適用する場合，基地局に到着したパケットの信号対干渉雑音電力 (SINR: Signal-to-Interference-plus-Noise Ratio) は基地局に近いユーザが遠いユーザと比較して高くなり復調が容易になると予測される．従来研究では，このような幾何学的配置構造を利用したプロトコルの設計はなされておらず，ユーザ全体で時間スロットあたりのパケットの送信確率を同一としている．本研究ではユーザが自身と基地局との距離を既知であるとし，パケットの送信確率を自律的に決定する距離を考慮した非正則フレームレス ALOHA(DIFA: Distance-aware Irregular Frameless ALOHA) を提案する．本論文では，提案方式である ZDCSA，E-ZDCSA，および DIFA が既存方式と比較して優れたスループット性能を達成することを数値解析より示す．

令和元年度　修士論文

Design and Analysis of Random Access Protocols Based on Successive Interference Cancellation and ZigZag Decoding

逐次干渉除去とZigZag復号に基づくランダムアクセスプロトコルの解析と設計

学籍番号　1831024

氏　　名　追永大

指導教員　石橋　功至 准教授

電気通信大学　情報理工学研究科

情報・ネットワーク工学専攻

提出日　令和2年3月17日

Design and Analysis of Random Access Protocols Based on Successive Interference Cancellation and ZigZag Decoding

Masaru Oinaga

Department of Computer and Network Engineering
The University of Electro-Communications

This dissertation is submitted for the degree of
Master in Engineering

March 2020

Acknowledgements

I would like to thank my supervisor, Associate Professor Koji Ishibashi, for his convincing guidance and ardent support which encouraged me throughout bachelor and master course at The University of Electro-Communications. I am also indebted to Professor Yasushi Yamao, Professor Takeo Fujii, and Associate Professor Koichi Adachi, for their insightful discussion. Moreover, I wish to acknowledge the support from my collegues of Advanced Wireless Communication Center. In addition, I express my gratitude to Dr. Shun Ogata for his help not only in research but also private life. Lastly, I would like to aknowledge the great love and support of my family. They kept me going on and hits work would have been impossible without their continuous help.

Masaru Oinaga
January 20th, 2020

Abstract

In this study, we investigated the effects of combining physical layer techniques for both framed and frameless ALOHA protocols with SIC. As for framed ALOHA, we investigated the effects of combining a zigzag decoder (ZD) with a coded ALOHA using the successive interference cancellation (SIC) technique to retrieve packets from collisions. We proposed *zigzag decodable coded slotted* ALOHA (ZDCSA) and *enhanced*-ZDCSA (E-ZDCSA) as a scheme which applies ZD before and after SIC, respectively. Furthermore, we derived the asymptotic analysis for the throughput and packet loss rate (PLR) performances of E-ZDCSA and validated its accuracy with the Monte Carlo simulations. Through numerical and asymptotic analyses, we showed that E-ZDCSA outperforms ZDCSA and the conventional coded ALOHA schemes in terms of throughput and PLR performances in most of the offered load regime. Moreover, we proposed *distance-aware irregular frameless* ALOHA (DIFA) as an enhanced protocol of conventional framless ALOHA. Based on the numerical analysis, we show that the proposed received-power-aware design of the transmission probability effectively improves the packet resolution probability and the throughput performances.

Table of contents

List of figures

List of tables

Nomenclature

Roman Symbols

d_i	Distance between i-th user and BS
d_{packet}	Duration of a packet
d_{prop}	Propagation delay
d_{slot}	Duration of a time slot
G	Offered load of the system
G^*	Offered load in which the throughput is maximized
$k_{\max}$	Maximum degree of degree distribution or probability mass function
$k_{\min}$	Minimum degree of degree distribution or probability mass function
L_k	Probability that user transmits k times within a time frame
$L(x)$	Distribution function of variable nodes
M	Number of time slots
N	Number of users
N_p	Number of segment which composes a packet
N_t	Number of segment which composes a time slot
$o_{i,j}$	j-th segment of the i-th observation node
O_j	j-th time slot or observation node
p	Transmission probability of a user per time slot

p_i Transmission probability of i-th user

$P(x)$ Probability mass function

q Probability that an edge is removed after successive interference cancellation

R Radius of the network

R_k Probability that k users simultaneously transmit within a time slot

$R(x)$ Distribution function of observation nodes

T_{ZD} Throughput when ZD is taken into consideration

u_i i-th user

V_i i-th user or variable node

$v_{i,j}$ j-th segment of the i-th variable node

Greek Symbols

α Ratio of the number of time slots added via the zigzag decoder to M

β Packet Loss Rate

$\Gamma_{i,t}$ Signal-to-interference-plus-noise ratio corresponding to the packet of i-th user transmitted in t-th time slot

λ_k Transmission probability of a user per time slot

ω Probability that the stopping set is successfully resolved by the zigzag decoder

ρ_k Transmission probability of a user per time slot

σ Thermal noise

Other Symbols

$\mathscr{O}$ Set consists of observation nodes

$\mathscr{U}_t$ Set of users transmitted in t-th time slot

$\mathscr{V}$ Set consists of variable nodes

Acronyms / Abbreviations

BS Base Station

CRDSA Contention Resolution Diversity Slotted ALOHA

DIFA Distance-aware Irregular Frameless ALOHA

E-ZDCSA Enhanced ZigZag Decodable Coded Slotted ALOHA

IoT Internet of Things

IRSA Irregular Repetition Slotted ALOHA

LDPC Low Density Parity Check

mMTC massive Machine Type Communications

MPR Multiple Packet Reception

PLR Packet Loss Rate

RA Random Access

SA Slotted ALOHA

SIC Successive Interference Cancellatiog

TDMA Time Division Multiple Access

ZDCSA ZigZag Decodable Coded Slotted ALOHA

ZD ZigZag Decoder

Chapter 1

Introduction

Due to the recent advances in the field of Internet of Things (IoT), a system composed of a massive number of devices connected via a wireless network is gathering attention. In particular, massive Machine Type Communications (mMTC) require extensive connectivity with the number of users in the system being more than 10^6 [2]. Further, the system is typically uplink-dominant, and the transmission of users are sporadic. Therefore, the design of a multiple access scheme which satisfies the requirements mentioned above is demanding.

The multiple access scheme can be categorized into two major types: grant access and random access (RA). The grant access scheme such as the time division multiple access (TDMA) is known to achieve high efficiency in terms of communication; however, an overhead of the resource allocation becomes critical when the network size is large. On the other hand, RA schemes such as pure ALOHA [3] does not allocate any resources and allows users to transmit at their own decision. Therefore, its overhead becomes much smaller compared to that of the resource allocation scheme. Nevertheless, when multiple packets arrive simultaneously at a receiver, this causes a collision of packets, thus, resulting in discarding of packets, which significantly limits the throughput performance of pure ALOHA. In [4], *Slotted* ALOHA (SA) has been proposed where users are time-synchronous, and each transmission is done within a time structure referred to as time slots. While SA improves the performance from the classical ALOHA, its peak throughput is still severely limited to $1/\mathrm{e} \approx 0.37$.

To conquer the problem of the packet collision, many of the proposed ALOHA protocols exploit the successive interference cancellation (SIC) as a technique for retrieving packets from the collision [5, 1, 6]. An ALOHA scheme with SIC is referred to as *coded* ALOHA, and among them, the contention resolution diversity slotted ALOHA (CRDSA) [5] is regarded as a milestone, which was originally proposed for satellite communications and later realized as a reasonable option for mMTC. In CRDSA, every user transmits its packet for a given

number of times within a time frame composed of several time slots. In [1], the irregular repetition slotted ALOHA (IRSA) was proposed as a generalization of CRDSA, where users individually determine the number of retransmissions based on a degree distribution. Moreover, an asymptotic analysis of the performance of IRSA based on a density evolution [7] was provided, which was inspired from graph-based codes such as low-density parity-check (LDPC) codes [8] and the peeling decoder [9]. It was shown that the IRSA achieved a high-throughput performance comparable with TDMA by optimizing the degree distribution via differential evolution [10]. However, the IRSA suffered from an extreme degradation of the throughput performance after its peak performance. This degradation is due to the limitation of SIC, where its decoding process only starts from packets without a collision, which the occurrence becomes rare in a high-load regime.

As another approach for resolving the collision of packets, a zigzag decoder (ZD) was proposed [11]. ZD was first proposed as a solution to the hidden terminal problem in IEEE 802.11 networks and was later applied to the ALOHA schemes [12–14]. In ZD, every packet is assumed to be equipped with a unique word or a *pilot* at both ends. This pilot enables the receiver to detect a time slot with the collision caused by two packets, if the packets are not completely over-wrapped. The receiver then immediately appends an additional time slot and requests the users who sent the packets to retransmit and other users to interrupt its transmission. This operation forms a set of collisions composed of packets from two different users. If the delay of the arrived packets is different between two patterns, ZD is able to retrieve the packets from both users. In [12], it was shown that ZD improved the throughput performance when it was applied to slotted ALOHA. As another example, the performance of the frameless ALOHA [15], a variant of the coded ALOHA inspired by the rateless codes [16], can also be enhanced with the application of ZD [14]. In both cases, it was pointed out that ZD is capable of suppressing the degradation of throughput after the peak. Hence, it is natural to think that ZD is expected to compensate for the problem of the coded ALOHA in the high-load regime. To the best of our knowledge, the performance analysis of a protocol which applies ZD into a framed coded ALOHA scheme has not yet been discussed.

In the case of framed ALOHA protocols mentioned above, the base station (BS) has to suitably select the number of time-slots, i.e., the time-frame length, before the transmission to achieve the designed throughput performance. If this length is inappropriate, the throughput performance significantly degrades from the designed value. To avoid the aforementioned degradation, *frameless ALOHA* has been proposed in [15]. In this protocol, each user transmits its packet based on a predefined transmission probability given by a *target degree*. The number of time-slots in the time-frame is not defined beforehand and is determined when

the number of resolved packets (users) exceeds the predefined threshold. Considering not only the collisions but also the received power of the transmitted packets, the multi-packet reception (MPR) via capture effect has been studied in [17]. This approach improves the throughput performance from the original frameless ALOHA, especially at a high-load region as the capture effect resolves some packets with a higher received power. Furthermore, if the above-mentioned capture effect is considered, it is natural to think that a user with a high received power is expected to be decoded first in a practical scenario. Hence, it is more efficient if a user with higher received power transmits its packet more frequently than a user with lower received power. This multi-slot type frameless ALOHA, where the transmission probability is not fixed among all users, was not considered in the past literature.

In this study, we propose several novel schemes for both framed and frameless ALOHA. For framed ALOHA, a zigzag decodable coded slotted ALOHA (ZDCSA) is proposed, where ZD is introduced to the coded ALOHA [1]. In ZDCSA, ZD is introduced before conducting SIC in order to reduce the number of packets that are not yet retrieved. Then, ZD is introduced after SIC in order to retrieve the remaining packets, which is referred to as *enhanced* ZDCSA (E-ZDCSA) in this study. The contributions of this study are summarized as follows:

- We discussed an approach referred to as ZDCSA, where ZD is applied before SIC. We also provided the optimization method of the degree distribution for ZDCSA.
- To improve the throughput performance, we proposed a novel scheme referred to as E-ZDCSA, in which ZD is applied after SIC. We also derived the theoretical performance of E-ZDCSA along with the optimization method of the degree distribution for E-ZDCSA.
- Based on the theoretical and numerical analyses, we showed that E-ZDCSA outperforms IRSA, especially in the high-load regime.

For frameless ALOHA, we propose a *distance-aware irregular frameless ALOHA* (DIFA) in which each user adjusts its transmission probability based on its received power at the BS to leverage the fact that users with a larger received power have higher chances of the correct reception. Specifically, we evaluate the effect of adjusting the transmission probability of each user based on the distance between user and BS. Through numerical results, it is shown that the performance can be improved by adjusting the transmission probability.

The remainder of this paper is organized as follows. In Chapter 2, a system model is provided. In Chapter 3, SIC is explained in detail, along with a bipartite graph representation. Chapter 4 describes ZD, followed by our proposed protocols and its optimization method in

Chapter 5. The numerical results on the throughput performance are presented in Chapter 6. The conclusions follow in Chapter 7.

Chapter 2

System Model

2.1 Network Model

In this study, a network model as shown in Fig. 2.1 is considered, where N users transmit their packets to a common receiver.

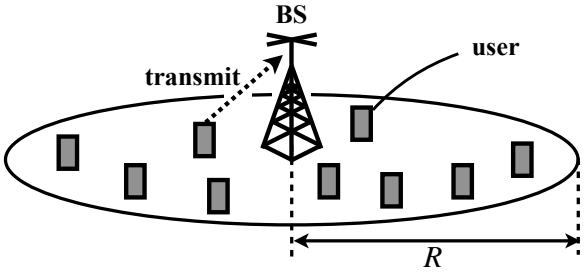

Fig. 2.1 Proposed system model. N users transmit packets to a common destination (receiver). Each user individually decides its transmission.

Additionally, all the transmissions are conducted within a time frame that is comprised of M time slots. Therefore, an offered load of the system is given by $G \triangleq N/M$. Every user and the receiver are assumed to be time-synchronous, and the packets are transmitted in a time slot domain. Each user also possesses a packet at the beginning and does not generate new packets during the transmission. If multiple packets simultaneously arrive at the receiver, all of them cannot be immediately retrieved due to packet collision.

2.1.1 Framed ALOHA

The collision at the receiver is considered the sole reason for packet loss, *i.e.,*the effects from a physical layer (*e.g.,*fading) is not considered. Moreover, multiple packet reception

(MPR) techniques such as exploiting capture effects [18] are also not considered, following a channel model proposed in [19].

Each packet is assumed to arrive at the receiver with a propagation delay within a guard interval installed in the time slot. Therefore, a relationship among the duration of the packet d_{packet}, the propagation delay d_{prop}, and the duration of the time slot d_{slot} is represented as $d_{\text{packet}} + d_{\text{prop}} \leq d_{\text{slot}}$. Besides that, the packet is assumed to be equipped with a unique word at both ends for user identification. This assumption is practical because the information of the transmitter should be included in each transmitted packet.

2.1.2 Frameless ALOHA

We assume a network with a circular Euclidean space of ${\mathbb{R}_+}^2$ [20], where radius is given by R [m]. The number of users denoted by N is a random variable that follows the Poisson distribution shown as

$$\Pr\left[N = k\right] = \frac{(\lambda S^2)^k \mathrm{e}^{-\lambda S^2}}{k!}, \tag{2.1}$$

where λ is a rate representing the expected number of users within a unit area, and $\Pr\left[x\right]$ represents the probability of a random variable x. The location of each user is uniformly chosen at random within the given network area, while BS is placed at the center. Note that N is assumed to be perfectly available at the BS. Moreover, both the user and BS are equipped with a single omnidirectional antenna.

Every packet sent from a user is disturbed by a path-loss and a frequency non-selective Rayleigh fading. The attenuation of the received power caused by the path-loss is given by

$$G_{\text{PL}}(d_i) = \frac{1}{1 + {d_i}^2}, \tag{2.2}$$

where d_i represents a distance between the i-th user, u_i, and the BS. This simple path-loss model is appropriate not only in the far-field but also in the near-field [21]. The fluctuation of the received power due to the Rayleigh fading follows an exponential distribution with mean = 1 given by

$$\Pr\left[G_{\text{R}} = x\right] = \mathrm{e}^{-x}. \tag{2.3}$$

With the above assumptions, the received power of the packet corresponding to u_i at the BS is given by

$$P_{\mathrm{r},i} = G_{\mathrm{PL}}(d_i) G_{\mathrm{R}} P_{\mathrm{t}}, \tag{2.4}$$

where P_{t} represents the transmission power.

2.2 Capture Effects

Let $\mathscr{U}_t$ denote a set of users which transmitted a packet at the t-th time-slot. The signal-to-interference-plus-noise ratio (SINR) corresponding to the packet sent by u_i at the t-th time-slot is given by

$$\Gamma_{i,t} \triangleq \frac{P_{\mathrm{r},i}}{\sum_{j \in \mathscr{U}_t \setminus i} P_{\mathrm{r},j} + \sigma^2}, \tag{2.5}$$

where σ^2 denotes the power of thermal noise. We assume that if $\Gamma_{i,t}$ exceeds a given threshold of Γ_{th}, it satisfies the inequality shown as

$$\Gamma_{i,t} > \Gamma_{\mathrm{th}}, \tag{2.6}$$

the packet of u_i arrived at the t-th time-slot would be successfully retrieved, which is called as the *capture effect*.

Chapter 3

Coded ALOHA

3.1 Irregular Repetition Slotted ALOHA

In this section, we briefly describe the conventional coded ALOHA scheme proposed in [1]. We first provide the assumption for the receiver, and then describe the graph representation of the relationship between the transmission of each packet and the observation at each time slot. Finally, we explain the asymptotic analysis and the optimization method for the conventional ALOHA scheme. Note that this chapter only considers MAC layer techniques.

First, the receiver is assumed to be able to distinguish the following states of each time slot:

1. *Idle*, where no users have transmitted.
2. *Singleton*, where only one user has transmitted.
3. Multiple users have transmitted, and packets collide.

The packet can be immediately retrieved if and only if it arrived at a singleton time slot. If a packet arrived at a time slot with a collision, it could not be retrieved unless:

1. the interference of other packets involved in the collision is removed and the time slot becomes singleton
2. the same packet which arrived at a different time slot is retrieved

3.1.1 Bipartite Graph Representation

The relationship between the transmission of a user and the observation at a time slot can be represented by a bipartite graph composed of *variable nodes*, *observation nodes*, and

edges. The variable node corresponds to the packet of each user, whereas the observation node corresponds to the packet reception at each time slot. In this study, a set consists of N variable nodes and M observation nodes which are denoted by $\mathscr{V}$ and $\mathscr{O}$, respectively. On the other hand, the edge corresponds to the relationship between each node, *i.e.,*if the i-th user has transmitted a packet to the j-th time slot, $V_i \in \mathscr{V}$ will be connected to $O_j \in \mathscr{O}$ with an edge. The number of edges connected to each node is referred to as a *degree*, and it represents the number of packet transmissions for variable nodes and the number of packet arrivals for observation nodes.

If a packet arrives at the time slot without a collision, it is assumed to be immediately retrieved. On the contrary, if multiple packets arrive simultaneously at the receiver, all of them cannot be retrieved unless an interference cancellation is performed. The coded ALOHA schemes proposed in [5, 1] utilized SIC after receiving M time slots. The decoding procedure of SIC can be described in a bipartite graph as such:

1. Search for an observation node with degree 1, which means a packet arrived at the corresponding time slot without a collision and thus can be immediately retrieved.

2. Track a variable node with the edge connected to the degree 1 observation node found in Step 1 and remove all the edges connected to that variable node.

3. Iterate Steps 1) and 2) until the number of observation nodes with degree 1 becomes 0.

Note that Step 2) leads to additional observation nodes with degree 1 and corresponds to removing the interference of a retrieved signal of the packet from other received signals at the time slot. Additionally, Step 2) is realized by assuming each packet is equipped with a pointer which indicates the time slot in which its replica was transmitted [5]. A dominant factor of the throughput degradation in a high-load regime is the rare occurrence of singleton observation nodes.

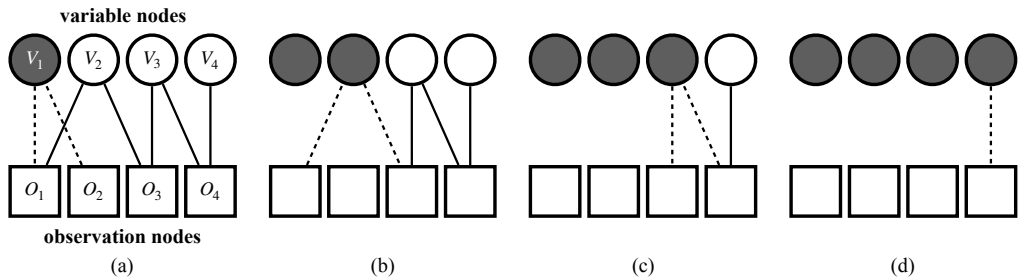

Fig. 3.1 Toy example of a bipartite graph where a set of variable nodes V_1, V_2, V_3 and V_4 are connected to observation nodes O_1, O_2, O_3 and O_4 with edges. Each variable node, observation node, and the edge is depicted as a circle, a square, and a line segment, respectively. The variable node is colored grey when the edges connected to that node is removed by SIC, *i.e.,* when the corresponding packet is retrieved.

The packet recovery via SIC can be explained using a toy example. The bipartite graph shown in Fig. 3.1 consists of a set of variable nodes $\mathscr{V} = \{V_1, V_2, V_3, V_4\}$, a set of observation nodes $\mathscr{O} = \{O_1, O_2, O_3, O_4\}$ and a number of edges that connect the nodes. (a) First, the edges connected to V_1 are removed as one of them is connected to O_2, which is a singleton node. (b) Next, the edges connected to V_2 are removed after O_1 becomes a singleton node. (c) Then, O_3 becomes a singleton node and thus enables the removal of the edges connected to V_3. (d) Finally, the edge connected to V_4 is removed, and SIC is terminated as the number of nodes with degree 1 became 0. Therefore, SIC can retrieve all the packets in the case of the toy example shown in Fig. 3.1.

3.1.2 Packet Loss Rate Analysis based on Density Evolution

Degree Distributions

In a system which adopts the IRSA approach, each user determines its packet transmission rate based on a given degree distribution function. Specifically, a user with degree-k selects k random time slots within the time frame. Let us denote the probability that the user transmits k times with L_k. Therefore, the degree distribution of the variable node is given by

$$L(x) \triangleq \sum_{k=1}^{k_{\max}} L_k x^k, \tag{3.1}$$

where $k_{\max}$ represents the maximum number of the packet transmissions and x is a dummy variable. The distribution, $L(x)$, is configurable by a system designer and is a target of optimization in order to achieve the highest peak throughput for a given $k_{\max}$. Note that the

IRSA is regarded as a generalization of CRDSA; CRDSA can be realized by setting

$$L_k = \begin{cases} 1 & (k = k_{\max}) \\ 0 & (\text{otherwise}) \end{cases}. \tag{3.2}$$

Similarly, the degree distribution of the observation node is given by

$$R(x) \triangleq \sum_{k=0}^{N} R_k x^k, \tag{3.3}$$

where R_k is the probability that the observation node has degree-k. Unlike $L(x)$, $R(x)$ cannot be configured by the system designer and depends on the realization of the system. However, each R_k can be calculated from a binomial distribution as follows:

$$R_k = \binom{N}{k} p^k (1-p)^{N-k}, \tag{3.4}$$

where p represents the transmission probability of a user per time slot, which is calculated as follows:

$$p = \frac{\sum_\ell \ell R_\ell}{N}. \tag{3.5}$$

When N, M is sufficiently large and p is very small, R_k can be approximated by Poisson distribution as

$$R_k \approx \frac{(\sum_\ell \ell R_\ell)^k \mathrm{e}^{-(\sum_\ell \ell R_\ell)}}{k!}. \tag{3.6}$$

From the definition, the average number of packet transmissions per user and packet arrivals per time slot is given by $\sum_k k L_k = L'(1)$ and $\sum_k k R_k = R'(1)$, respectively, where $(\cdot)'$ represents the first-order derivative. Therefore, the offered load of the system can be written as $G = N/M = R'(1)/L'(1)$.

Moreover, the *edge-perspective* degree distribution can be defined by considering the probability of the edge connected to a node with degree-k. Let the probability of an edge connected to a variable node with degree-k be denoted by λ_k. Similarly, the probability of an edge connected to an observation node with degree-k can be denoted by ρ_k. If L_k and R_k are given, then λ_k and ρ_k can be defined as

$$\lambda_k \triangleq \frac{L_k k}{\sum_\ell \ell L_\ell} \tag{3.7}$$

and

$$\rho_k \triangleq \frac{R_k k}{\sum_\ell \ell R_\ell}, \tag{3.8}$$

respectively. Then, the edge-perspective degree distribution functions for the variable and observatin nodes can be given by

$$\lambda(x) \triangleq \sum_{k=1}^{k_{\max}} \lambda_k x^{k-1} \tag{3.9}$$

and

$$\rho(x) \triangleq \sum_{k=1}^{N} \rho_k x^{k-1}, \tag{3.10}$$

respectively.

Density Evolution

The theoretical analysis of the packet loss rate (PLR) of the coded ALOHA can be performed with density evolution [22] which involves iterative calculation over the aforementioned degree distributions. Let q_i denote the probability that the edge is connected to an observation node and not yet removed in the i-th iteration. With the distribution functions given by Eqs. (3.9) and (3.10), q_i is given by

$$q_i = \sum_{k=1}^{N} \rho_k \big(1 - (1 - \lambda(q_{i-1}))^{k-1}\big) \tag{3.11}$$

$$= 1 - \rho\big(1 - \lambda(q_{i-1})\big), \tag{3.12}$$

where $q_0 = 1$. For the sake of notation simplicity, the index of q_i will be dropped and be denoted by q for the rest of this paper. After q is sufficiently updated with Eq. (3.12), the resulting PLR is calculated by substituting q for $L(x)$ in Eq. (3.1). Although this theoretical analysis considers an asymptotic setting where N and M are both infinite, it is still useful for an analysis of the practical settings [1].

3.1.3 Optimization of Degree Distribution

For each value of the offered load G, $R(x)$ and $\rho(x)$ can be derived from $L(x)$ and $\lambda(x)$. Therefore, if G and $L(x)$ are given, the probability q can be derived via the density evolution

Table 3.1 Optimized degree distributions for $k_{\max} = 4, 5, 6, 8$ provided in [1].

$k_{\max}$	$L(x)$	$T(L(x))$
4	$0.5102x^2 + 0.4898x^4$	0.868
5	$0.5631x^2 + 0.0436x^3 + 0.3933x^5$	0.898
6	$0.5465x^2 + 0.1623x^3 + 0.2912x^6$	0.915
8	$0.5x^2 + 0.28x^2 + 0.22x^8$	0.938

given by Eq. (3.12). Then, the offered load G^* in which the throughput is maximized can be derived from

$$\max_{G} \; G \times \big(1 - L(q)\big) \tag{3.13}$$

$$\text{s.t. } G > 0, \tag{3.14}$$

where q is the result of density evolution. Then, the peak throughput, when $L(x)$ is given, can be defined by the following function

$$T\big(L(x)\big) \triangleq G^* \times \big(1 - L(q)\big). \tag{3.15}$$

The optimum $L(x)$ for each $k_{\max}$ can be obtained from

$$\max_{L(x)} \; T(L(x)) \tag{3.16}$$

$$\text{s.t. } \sum_{k=1}^{k_{\max}} L_k = 1. \tag{3.17}$$

Note that the optimization problem given by Eqs. (3.16) and (3.17) can be solved by differential evolution [10]. Differential evolution is a meta-heuristic algorithm composed of iterative process of combining sufficient number of candidates and swapping the coefficients based on evaluation result. In this paper, we denote the number of candidates by N_{cands}. Also, the mutation factor denoted by μ is introduced to indicate how radical mutation is operated during generating mutant of a candidate. In Table 3.1, the optimized degree distributions derived in [1] are provided.

3.2 Frameless ALOHA

In this section, frameless ALOHA with and without the capture effect [15, 17] are briefly explained as the conventional protocol.

For performance parameters of interest, the probability of packet resolution, P_{R}, is defined by the number of resolved users divided by that of all users, and the throughput, T, is calculated by

$$T = \frac{P_{\mathrm{R}}}{M/N}, \tag{3.18}$$

where M is defined by the length of the time-frame when it is terminated.

In frameless ALOHA, every user has a transmission probability p at the beginning of the time-frame. Based on p, a user determines whether they transmit at each time-slot. This probability is calculated by the number of users, N, as given by

$$p = \frac{\beta}{N}, \tag{3.19}$$

where β is called a *target degree*, which represents the expected number of arriving packets per time-slot. To maximize performance of the packet resolution, P_{R}, and throughput, T, β must be optimized for the given N and M.

The time-frame is terminated when P_{R} exceeds the pre-defined threshold, P_{th}. The probability that user u_i transmits packet m times within M time-slots is given by a binomial distribution shown as

$$\Pr\left[x = m\right] = \binom{M}{m} p^m (1-p)^{M-m}. \tag{3.20}$$

As some users might not transmit within the time-frame, there exists an error floor in terms of P_{R} [15, 16].

Chapter 4

ZigZag Decoder

As mentioned in the previous section, SIC requires a singleton node in order to start its decoding process. Therefore, if a transmission is done in a manner shown in the bipartite graph in Fig. 4.1(a), SIC cannot retrieve the packets anymore. The realization of the bipartite graph without the singleton observation nodes is referred to as a *stopping set*, which is regarded as a significant reason behind the degradation of throughput in a high-load regime. In this paper, we refer to the bipartite graph in Fig. 4.1(a) as the stopping set unless otherwise specified.

On the other hand, the zigzag decoder (ZD) proposed in [11] has a chance of resolving the stopping sets such as Fig. 4.1(a). When considering ZD, each time slot will be further divided into *segments*, and supposes that the packet arrives at the time slot with a *segment-wise* propagation delay. Then, the receiver is capable of distinguishing the following states of each time slot:

1. *Idle*, where no users have transmitted.
2. *Singleton*, where only one user has transmitted.
3. Two users have transmitted, and packets have collided.
4. More than two users have transmitted, and packets have collided.

Note that State 3) is only distinguishable if two packets arrive with a different propagation delay and are not completely overlapped [11]. If State 3) occurs at the time slot, the receiver immediately appends an additional time slot. Then, the receiver broadcasts a signal to request the user to retransmit its packet at the additional time slot if it transmitted at the most recent time slot. If only the requested users transmit their packet at the additional time slot, a stopping set as shown in Fig. 4.1(a) can be manually formed. Then, ZD will perform a

segment-wise interference cancellation over the stopping set. In this study, the two packets involved in the stopping set are retrieved with a probability of ω. Note that $(1-\omega)$ includes the probability that the arrived two packets were overlapped entirely, and therefore, the segment-wise SIC could not be applied.

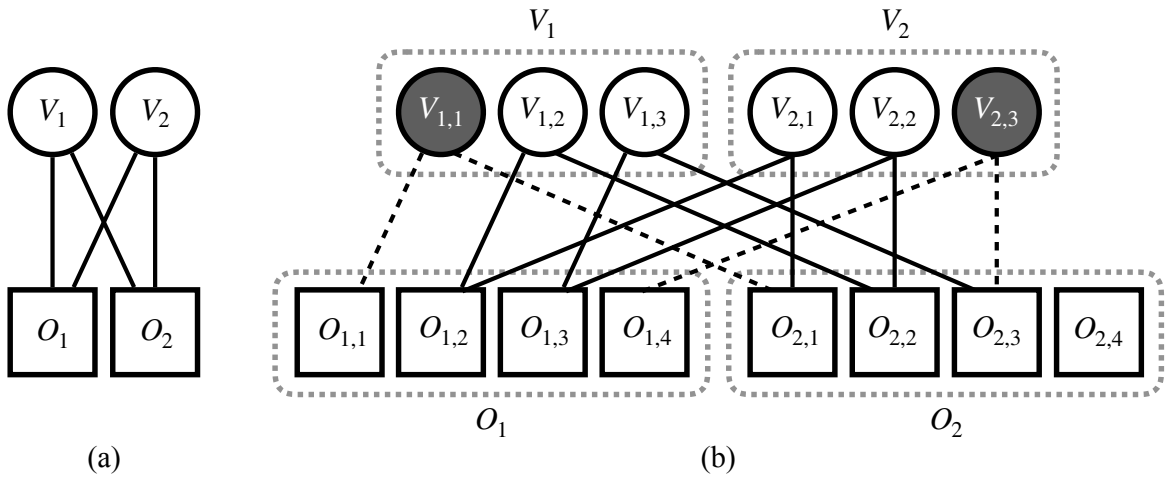

Fig. 4.1 Toy example of a bipartite graph of a stopping set composed of two variable nodes, V_1, V_2, and two observation nodes O_1, O_2.

The decoding process of ZD can be regarded as a segment-wise SIC, which can be explained using the bipartite graph. Suppose that the packet and the time slot is composed of N_p and N_t segments respectively, then, the variable node corresponding to the i-th user can be decomposed into $V_i = \{v_{i,j} \mid 0 \leq j \leq N_p\}$. Similarly, the observation node corresponding to the i-th time slot can be decomposed into $O_i = \{o_{i,j} \mid 0 \leq j \leq N_t\}$. Fig. 4.1(b) shows an example with $N_p = 3$ and $N_t = 4$, where each node is decomposed into $V_1 = \{V_{1,1}, V_{1,2}, V_{1,3}\}$, $V_2 = \{V_{2,1}, V_{2,2}, V_{2,3}\}$, $O_1 = \{O_{1,1}, O_{1,2}, O_{1,3}, O_{1,4}\}$, and $O_2 = \{O_{2,1}, O_{2,2}, O_{2,3}, O_{2,4}\}$. The decoding process is initiated by retrieving segments $V_{1,1}$ and $V_{2,3}$ which arrive respectively at the singleton segments $O_{1,1}$ and $O_{1,4}$. After removing the interference of $V_{1,1}$ and $V_{2,3}$ from all the other segments, segments $O_{2,1}$ and $O_{2,3}$ become singleton. Then, segments $V_{1,3}$ and $V_{2,1}$ can be retrieved respectively from the singleton segments $O_{2,1}$ and $O_{2,3}$. Finally, segments $V_{1,2}$ and eventually $V_{2,2}$ can be retrieved after the interference cancellation. Therefore, all the segments of both V_1 and V_2 can be retrieved via ZD in this example.

Chapter 5

Proposed Protocols

In this section, a combination of the zigzag decoder and the conventional coded ALOHA scheme is considered.

5.1 ZDCSA

In ZDCSA, the receiver changes its behavior only if two packets arrived at the same time slot, and otherwise operate similarly with IRSA. Moreover, based on the state of the time slot, the receiver successively operates while receiving packets. When State 3) shown in the previous section occurs, the receiver appends a time slot immediately afterward and requests users who sent the packet to retransmit their packet. The requested packet retransmission is done in the appended time slot, where the left of the users halt their transmission until the retransmission is completed. Thus, the stopping set is manually created, where involved packets can be retrieved via ZD with the probability of ω. If packets are successfully retrieved, the transmitters of that packet halt its packet transmission for the left of the time frame. The time frame is terminated if the receiver received M time slots without counting the appended time slots.

In order to consider the overhead of ZD, we defined the ratio of the number of time slots added via the ZD to M as α. Therefore, we redefined the throughput calculation as

$$T_{\mathrm{ZD}} \triangleq \frac{G}{1+\alpha} \times (1-\beta) \tag{5.1}$$

where β represents PLR. Furthermore, the peak throughput when $L(x)$ is applied is denoted by $T_{\mathrm{ZD}}(L(x))$. Note that for schemes without ZD, such as the IRSA and CRDSA, α is set to 0.

Table 5.1 Optimized distribution function for ZDCSA in case of $k_{\max} = 4,5,6,8$.

$k_{\max}$	$L(x)$
4	$0.3761x^2 + 0.0683x^3 + 0.5556x^4$
5	$0.4162x^2 + 0.0852x^3 + 0.2170x^4 + 0.2816x^5$
6	$0.4677x^2 + 0.0296x^4 + 0.1646x^5 + 0.2524x^6$
8	$0.4280x^2 + 0.1999x^3 + 0.0523x^4$ $+0.0071x^5 + 0.0223x^6 + 0.2016x^7 + 0.0888x^8$

Unlike the conventional coded ALOHA, ZDCSA is incapable of strict analysis based on density evolution. The problem of analytical tractability is caused by whether the ZD event that occurs at a particular time slot depends on the previous slots to that time slot. Therefore, the degree distribution for ZDCSA is optimized to maximize the peak throughput in a finite setting. The optimization problem can be written as

$$\max_{L(x)} \; T^{\mathrm{ZD}}(L(x)) \tag{5.2}$$

$$\text{s.t.} \sum_{k=0}^{k_{\max}} L_k = 1, \tag{5.3}$$

where $T^{\mathrm{ZD}}(L(x))$ in this study was obtained from the Monte Carlo simulation with $N = 10^4$. In Table 5.1, the results of the optimization via differential evolution for $k_{\max} = 4,5,6,8$ are presented.

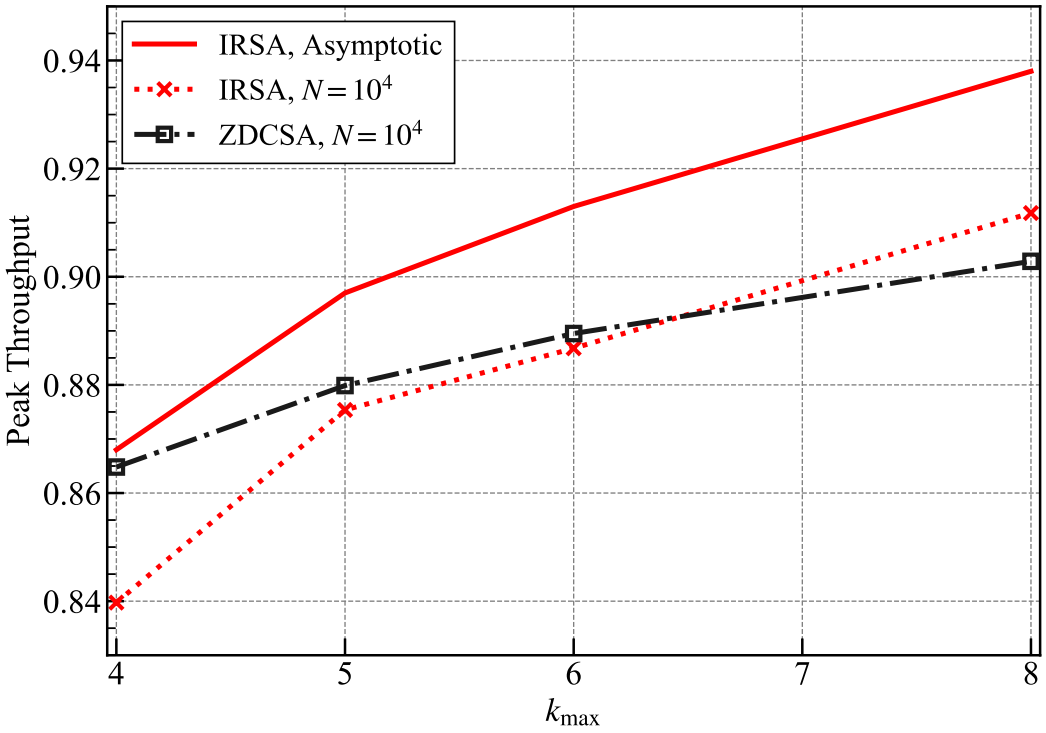

Fig. 5.1 Peak throughput comparison between IRSA and ZDCSA with $k_{\max} = 4,5,6,8$.

The peak throughput comparison between the IRSA and ZDCSA with $k_{\max} = 4,5,6,8$ is presented in Fig. 5.1. As seen in the figure, the peak throughput performance of the IRSA and ZCDSA improves as $k_{\max}$ increases. The figure also reveals that the IRSA outperforms ZDCSA when $k_{\max}$ becomes 8 or in the asymptotic setting. This outcome is due to two reasons:

1. The degree distribution of the IRSA is optimized via an asymptotic setting. The optimization $L(x)$ for ZDCSA is done in a non-asymptotic setting *i.e.,*when N becomes large, the IRSA will eventually outperform ZDCSA in terms of peak throughput.

2. Time slots are added excessively by the ZD, even in a load region where SIC is capable of retrieving packets of all the users.

Therefore, a scheme which achieves the performance comparable to the IRSA with less addition of time slots is required.

5.2 E-ZDCSA

Next, another novel approach referred to as the *enhanced*-ZDCSA (E-ZDCSA) is proposed. In E-ZDCSA, the packet transmission and packet recovery is first conducted in an IRSA

manner. Within the received time frame, the receiver first appends time slot if it detects the time slot with a collision caused by two packets. Then, it addresses the transmitter of the packets involved in the collided time slot to retransmit its packet to the appended time slot in order to form the stopping set. Finally, the stopping set is resolved via ZD with a probability of ω. As ZD is operated if SIC could not resolve a collision of packets, E-ZDCSA enables a decrease in the number of appended time slots compared to ZDCSA. Furthermore, E-ZDCSA is capable of optimizing its performance via asymptotic analysis based on density evolution.

5.2.1 Asymptotic Analysis based on Density Evolution

First, the node-perspective degree distributions after SIC are derived in order to track the asymptotic performance of E-ZDCSA. Let L_k^{SIC} denote the probability that a variable node has degree-k after SIC. L_k^{SIC} can be derived by $L_k^{\mathrm{SIC}} = l_k / \sum_\ell l_\ell$, where l_k $(k \geq 0)$ is calculated by

$$l_k = \begin{cases} 1 - \sum_{\ell=1} L_\ell q^\ell & (k=0) \\ L_k q^k & (k>0) \end{cases}, \tag{5.4}$$

and q is the result of density evolution given by Eq. (3.12).

In the same manner as L_k^{SIC}, let R_k^{SIC} denote the probability that an observation node has degree-k after SIC. R_k^{SIC} can be derived by $R_k^{\mathrm{SIC}} = r_k / \sum_\ell r_\ell$, where r_k $(k \geq 0)$ is calculated by

$$r_k = \begin{cases} \displaystyle\sum_{m=0}^{1} \sum_{\ell=m}^{N} R_\ell \binom{\ell}{m} \lambda(q)^m (1-\lambda(q))^{\ell-m} & (k=0) \\ 0 & (k=1) \\ \displaystyle\sum_{\ell=k}^{N} R_\ell \binom{\ell}{k} \lambda(q)^k (1-\lambda(q))^{\ell-k} & (k>1) \end{cases}. \tag{5.5}$$

From the above definitions, the degree distributions of a variable and an observation node after SIC can be defined as

$$L^{\mathrm{SIC}}(x) \triangleq \sum_{k=0}^{k_{\max}} L_k^{\mathrm{SIC}} x^k \tag{5.6}$$

and

$$R^{\mathrm{SIC}}(x) \triangleq \sum_{k=0}^{N} R_k^{\mathrm{SIC}} x^k, \tag{5.7}$$

Table 5.2 Optimized degree distributions for E-ZDCSA in case of $k_{\max} = 4, 5, 6, 8$.

$k_{\max}$	$L(x)$	$T(L(x))$
4	$0.5130x^2 + 0.0013x^3 + 0.4857x^4$	0.8682
5	$0.5630x^2 + 0.0413x^3 + 0.3956x^5$	0.8977
6	$0.5485x^2 + 0.1389x^3 + 0.0276x^4$ $+0.0168x^5 + 0.2682x^6$	0.9130
8	$0.5116x^2 + 0.2633x^3 + 0.0003x^4 + 0.0019x^5$ $+0.0048x^6 + 0.0405x^7 + 0.1776x^8$	0.9381

respectively. Next, let λ_k^{SIC}, ρ_k^{SIC} denote the probability that an edge is connected to a degree-k variable and observation node, respectively. From L_k^{SIC} and R_k^{SIC}, λ_k^{SIC} and ρ_k^{SIC} can be derived by

$$\lambda_k^{\mathrm{SIC}} \triangleq \frac{L_k^{\mathrm{SIC}} k}{\sum_\ell \ell L_\ell^{\mathrm{SIC}}} \tag{5.8}$$

and

$$\rho_k^{\mathrm{SIC}} \triangleq \frac{R_k^{\mathrm{SIC}} k}{\sum_\ell \ell R_\ell^{\mathrm{SIC}}}, \tag{5.9}$$

respectively. Then, the edge-perspective degree distributions after SIC are given by

$$\lambda^{\mathrm{SIC}}(x) \triangleq \sum_{k=1}^{k_{\max}} \lambda_k^{\mathrm{SIC}} x^{k-1} \tag{5.10}$$

and

$$\rho^{\mathrm{SIC}}(x) \triangleq \sum_{k=1}^{N} \rho_k^{\mathrm{SIC}} x^{k-1}, \tag{5.11}$$

respectively. When ZD is utilized, the edges connected to an observation node with degree-2 can be removed with a probability of ω. Hence, the probability that an edge is not removed after ZD is derived from

$$q^{\mathrm{ZD}} \triangleq q(1 - \omega \rho_2^{\mathrm{SIC}}). \tag{5.12}$$

Therefore, the PLR after ZD can be calculated by $L(q^{\mathrm{ZD}})$.

5.2.2 Optimization of $L(x)$ in case of E-ZDCSA

In the same manner as IRSA, the offered load $G^\star$ in which the throughput is maximized can be derived by

$$\max_{G} \; G \times \left(1 - L(q^{\mathrm{ZD}})\right) \tag{5.13}$$

$$\text{s.t. } G > 0. \tag{5.14}$$

Then, the peak throughput of E-ZDCSA when $L(x)$ is given can be defined by the following function:

$$T^{\mathrm{E-ZD}}\big(L(x)\big) \triangleq \frac{G^\star}{1+\alpha} \times \left(1 - L(q^{\mathrm{ZD}})\right). \tag{5.15}$$

Therefore, the optimum $L(x)$ for each $k_{\max}$ can be obtained from

$$\max_{L(x)} \; T^{\mathrm{E-ZD}}(L(x)) \tag{5.16}$$

$$\text{s.t. } \sum_{k=1}^{k_{\max}} L_k = 1. \tag{5.17}$$

In the same manner as IRSA, degree distributions for E-ZDCSA is optimized via differential evolution. Fig. 5.2 shows the improvements of throughput performance via differential evolution in the case of $N_{\mathrm{cand}} = 10^3$, $\mu = 0.8$, and $k_{\max} = 8$. In Table 5.2, the results of optimization via differential evolution for $k_{\max} = 4, 5, 6, 8$ are presented.

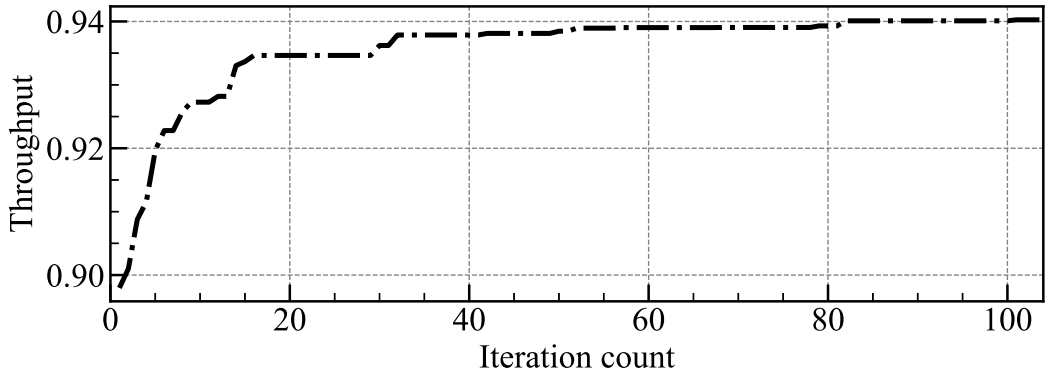

Fig. 5.2 The throughput performance improvements via differential evolution in the case of $N_{\mathrm{cand}} = 10^3$, $\mu = 0.8$, and $k_{\max} = 8$.

Note that the IRSA and E-ZDCSA share the same peak throughput performance when the utilized degree distribution $L(x)$ is the same.

5.3 Distance-aware Irregular Frameless ALOHA

In this section, we present a novel protocol, which is referred to as *distance-aware irregular frameless ALOHA* (DIFA). Intuitively, packets with higher received-power at the BS are likely to be recovered first when the capture effect is applied as a means to retrieve packets from a collision. Based on the aforementioned insight, we introduce the probability mass function (pmf) in order to determine the transmission probability of a user based on its location.

Let us denote the maximum and minimum degree of pmf by $k_{\max}$ and $k_{\min}$, respectively. Then, the probability mass function in this paper is given by a polynomial form of

$$P(x) \triangleq \sum_{k=k_{\min}}^{k_{\max}} P_k x^k, \tag{5.18}$$

where P_k, x denotes the probability that the user selects k-th group, and dummy variable, respectively.

Let us suppose that user u_i has a knowledge of S, $P(x)$, and d_i. Then, the transmission probability of u_i is determined by

$$p_i \triangleq \begin{cases} p & \left(1 - P_{k_{\min}} < \left(\frac{d_i}{S}\right)^2\right) \\ \vdots & \\ \frac{k}{k_{\min}} \cdot p & \left(\sum_{\ell=k+1}^{k_{\max}} P_\ell \leq \left(\frac{d_i}{S}\right)^2 < \sum_{\ell=k}^{k_{\max}} P_\ell\right), \\ \vdots & \\ \frac{k_{\max}}{k_{\min}} \cdot p & \left(\left(\frac{d_i}{S}\right)^2 < P_{k_{\max}}\right) \end{cases} \tag{5.19}$$

where only k with $P_k \neq 0$ is considered. This formula is based on the insight that users are likely to have a higher received-power if they are closer to the BS and, thus, should be given a higher transmission probability. Note that $p = \beta/N$ is optimized to achieve the highest peak throughput for a given probability mass function $P(x)$. Therefore, unlike the conventional schemes [15, 17], the transmission probability is no longer shared among all users.

Furthermore, let us define the group in which i-th user u_i belongs to as g_i, determined by

$$g_i \triangleq \begin{cases} G_{k_{\min}} & \left(1 - P_{k_{\min}} < \left(\frac{d_i}{S}\right)^2\right) \\ \vdots & \\ G_k & \left(\sum_{\ell=k+1}^{k_{\max}} P_\ell \leq \left(\frac{d_i}{S}\right)^2 < \sum_{\ell=k}^{k_{\max}} P_\ell\right), \\ \vdots & \\ G_{k_{\max}} & \left(\left(\frac{d_i}{S}\right)^2 < P_{k_{\max}}\right) \end{cases} \tag{5.20}$$

where only k with $P_k \neq 0$ is considered. As seen from the equation, user which belongs to G_k has a transmission probability of $\frac{k}{k_{\min}} \cdot p$. Also, $G_{k_{\min}}$ and $G_{k_{\max}}$ represents the furthest and closest group of users, respectively.

5.3.1 Optimization of $P(x)$ in case of DIFA

Because of its low analytical tractability due to a complex structure and the number of parameters being large, DIFA is incapable of strict analysis based on density evolution. Therefore, in the same manner with ZDCSA, $P(x)$ is optimized via differential evolution [10] to achieve the highest throughput performance for a given $k_{\max}$ and $k_{\min}$.

Chapter 6

Numerical Analysis

In this chapter, proposed schemes are compared with conventional schemes via numerical analyses. Note that for every differential evolution, mutation factor and the number of candidates is set to 0.8 and 10^2, respectively.

6.1 ZDCSA and E-ZDCSA

In this section, the performance of our proposed protocols are compared with the conventional coded ALOHA schemes. First, the accuracy of the proposed node distribution analysis provided in Section IV is validated. Then, the throughput and PLR performances of ZDCSA and E-ZDCSA are compared to that of the conventional IRSA. Finally, the analysis when ω is altered is provided.

6.1.1 Distributions after SIC

In this section, the theoretical and simulation results of node distribution after SIC are compared. In order to measure the difference between the distributions, the Kullback-Leiber (KL) divergence [23] denoted by $D_{\mathrm{KL}}(P||Q)$ is introduced, where P and Q are both a discrete probability mass function (PMF). In this study, P and Q are derived via the asymptotic and numerical analysis, respectively.

Fig. 6.1 shows the result of the KL divergence when comparing the theoretical and numerical results of the distribution of the variable and observation node after SIC.

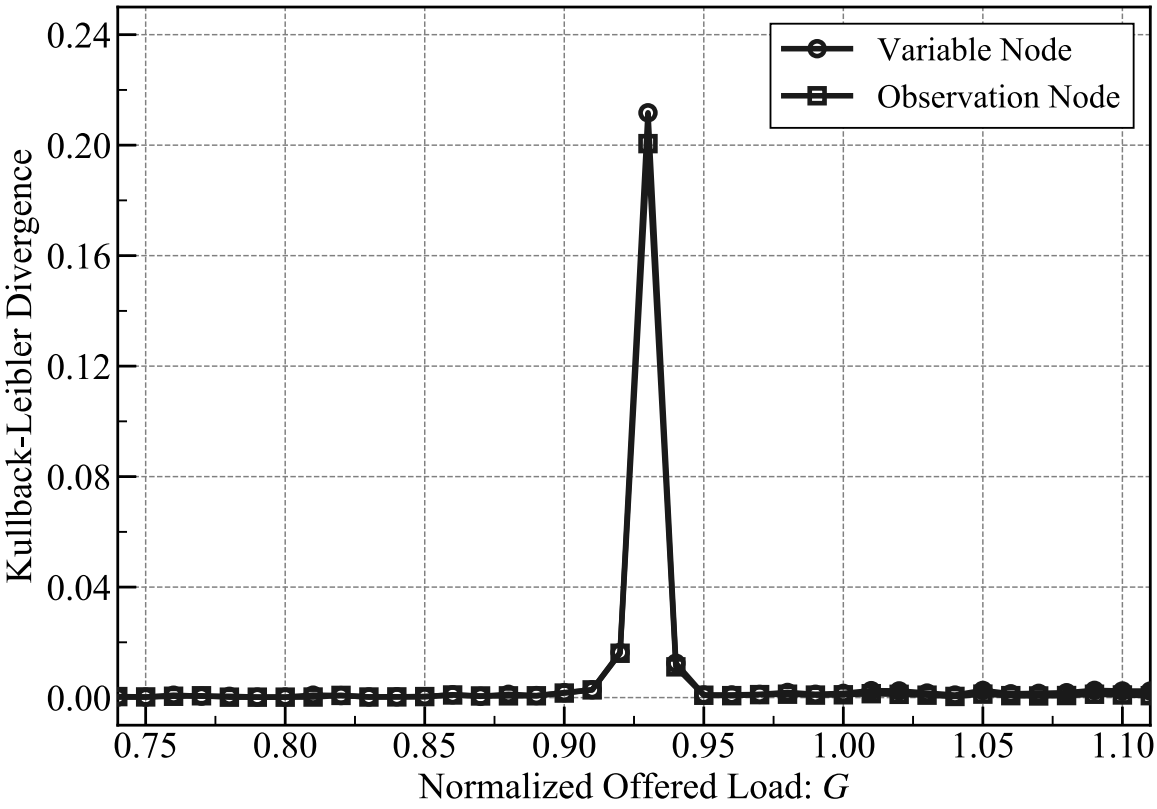

Fig. 6.1 The KL divergence when comparing the theoretical and numerical results of the variable and observation node distribution after SIC.

For both the asymptotic and simulation settings, the node distribution $L(x)$ is set as

$$L(x) = 0.5x^2 + 0.28x^3 + 0.22x^8, \tag{6.1}$$

and $N = 10^4$ for the Monte Carlo simulation. From the result shown in Fig. 6.1, the theoretical analysis proposed in this study enables the node distributions after SIC to be tracked in most cases except in the moderate-to-high load regime, or the so-called *waterfall region*. Although a finite analysis of IRSA in the waterfall region is provided in [24], it is not introduced in this study for the sake of simplicity.

6.1.2 Throughput and PLR Performances

Next, the throughput and PLR performances of the proposed schemes (ZDCSA and E-ZDCSA) are compared with the conventional scheme (IRSA). The node distribution $L(x)$ is

set as

$$L(x) = 0.5116x^2 + 0.2633x^3 + 0.0003x^4 + 0.0019x^5 + 0.0048x^6 + 0.0405x^7 + 0.1776x^8, \tag{6.2}$$

for IRSA and E-ZDCSA, and

$$L(x) = 0.4280x^2 + 0.1999x^3 + 0.0523x^4 + 0.0071x^5 + 0.0223x^6 + 0.2016x^7 + 0.0888x^8 \tag{6.3}$$

for ZDCSA. Further, N is set to 10^4 for a non-asymptotic setting.

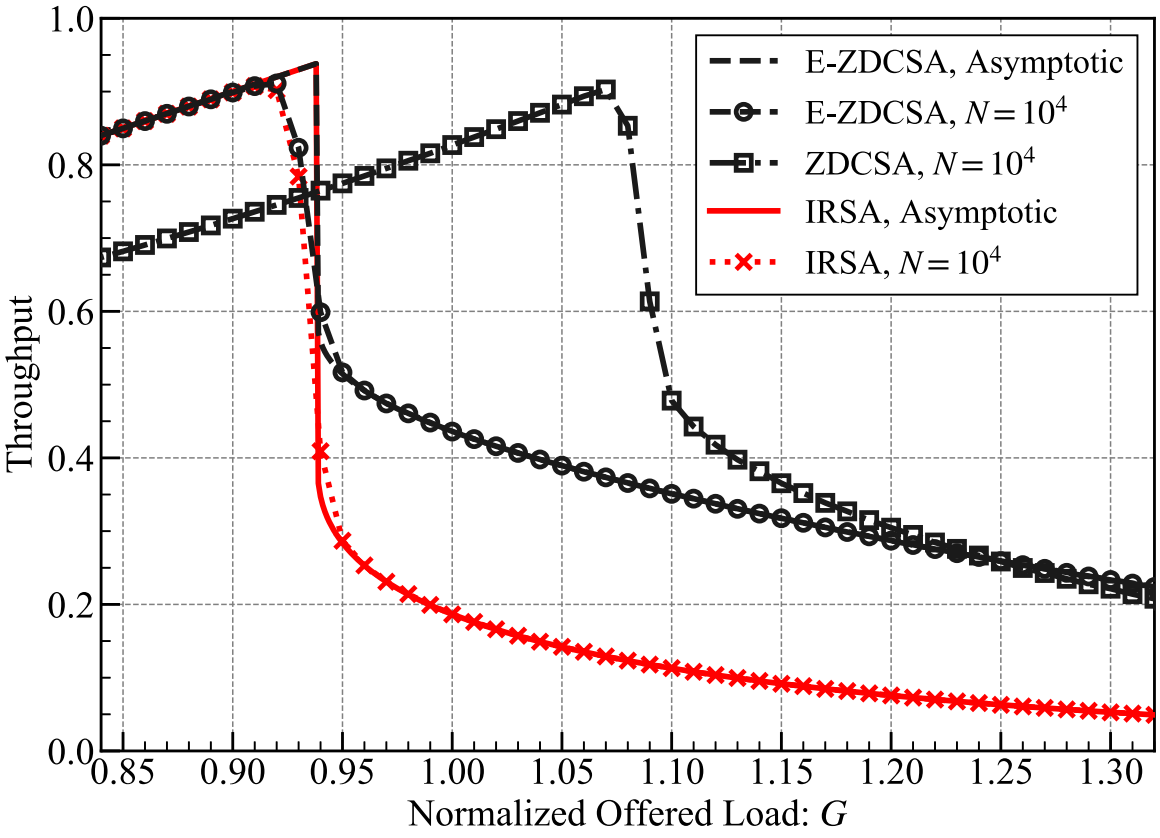

Fig. 6.2 Throughput performances of IRSA, ZDCSA, and E-ZDCSA.

As seen from Fig. 6.2, both the proposed schemes with ZD clearly suppressed the degradation of the throughput performance in a high-load regime compared to the conventional IRSA. Besides that, the effect of the overhead caused by appending time slots via ZD is significantly depicted in the result of ZDCSA; although the peak throughput was relatively high, its throughput performance was degraded in a moderate-load regime. On the other hand,

E-ZDCSA showed a throughput performance similar to that of IRSA, where the throughput rises linearly to N/M until its peak. After its peak, E-ZDCSA outperformed the IRSA thanks to ZD, and eventually, ZDCSA because of less overhead. In the peak throughput performance comparison, both E-ZDCSA and IRSA achieved 1.0381 in the asymptotic setting. For non-asymptotic setting with $N = 10^4$, the peak throughputs of IRSA, ZDCSA, and E-ZDCSA were 1.0045, 1.0029 and 1.0056, respectively. Therefore, it can be deduced that E-ZDCSA is the most effective scheme in terms of throughput performance.

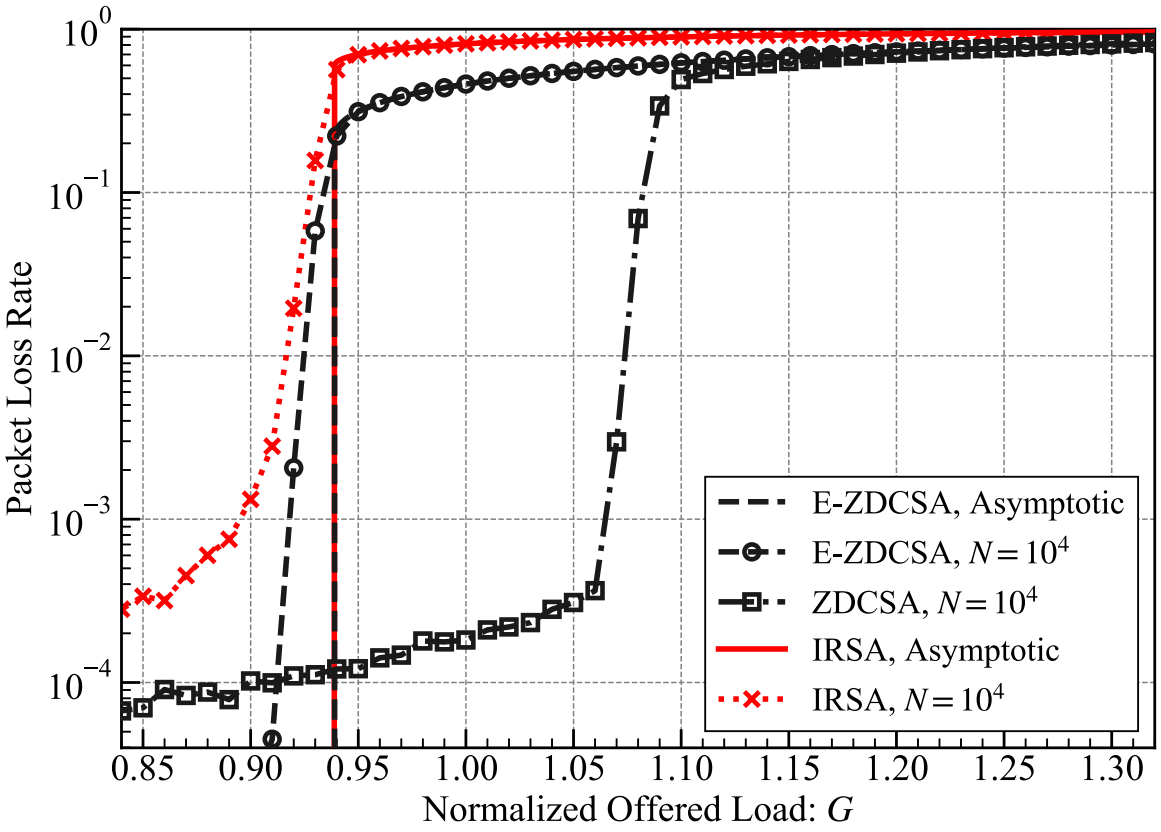

Fig. 6.3 PLR performances of IRSA, ZDCSA, and E-ZDCSA.

From Fig. 6.3, it can be seen that E-ZDCSA and IRSA did not have an error floor in the asymptotic setting. Conversely, in the non-asymptotic setting, the proposed schemes showed a lower error floor compared to IRSA. Notably, E-ZDCSA drew its error floor lower than the other two schemes and achieved the lowest PLR in the region of $G \leq 1.01$. While the offered load G was in the range of $[1.01, 1.23]$, ZDCSA showed the lowest PLR owing to the structure of applying ZD before SIC. After G became higher than 1.23, E-ZDCSA outperformed ZDCSA by achieving the lowest PLR among all the schemes in comparison. Therefore, it can be concluded that E-ZDCSA is the most effective scheme in almost all the load regimes in terms of PLR performance.

For both throughput and PLR analyses, the results of the Monte Carlo simulation validated the asymptotic analysis presented in the previous chapter.

6.1.3 Throughput Performance in a Practical Scenario

Finally, this section observes the peak throughput performance of the proposed schemes when ZD success probability ω is changed. As the transmission of users is typically sporadic [2] in the mMTC scenario, the number of active users is assumed to be relatively small compared to the number of all users. Therefore, this section considered a smaller number of users compared to the previous analyses. As described in Section IV, ZD can be applied if two packets arrived with a different propagation delay. For simplicity, the delay of the packet of each user can be regarded as a random selection of back-off patterns. Then, it can be said that the ZD fails only if two users picked the same back-off pattern. Therefore, the ZD success probability can be calculated as

$$\omega = 1 - N_{\mathrm{B}}^{-1}, \tag{6.4}$$

where N_{B} denotes the number of back-off patterns.

Fig. 6.4 shows the peak throughput performance comparison of IRSA, ZDCSA and E-ZDCSA in $\omega \in [0,1]$ when N is set to 10^4. Note that the node distribution is configured according to Eq. (6.2) for IRSA and E-ZDCSA, and Eq. (6.3) for E-ZDCSA. From the result of $\omega = 0$, it can be seen that E-ZDCSA significantly decreased the number of appending time slots compared to ZDCSA. For E-ZDCSA, it outperformed IRSA when ω was greater than 0.5. Therefore, only $(1-\omega)^{-1} = 2$ back-off patterns were required in order for E-ZDCSA to achieve better performance than the conventional IRSA. In the case of ZDCSA, it outperformed IRSA with $\omega \geq 1.0$, meaning that the number of back-off patterns in order to outperform IRSA was approximately 10. In particular, N_{B} was initialized to 32 in IEEE 802.11 [11], which yielded $\omega = 1 - 32^{-1} \approx 1.069$. As shown in the figure, both ZDCSA and E-ZDCSA outperformed the IRSA when ω was set to 1.069. Therefore, the proposed protocols are effective in terms of the practical scenario.

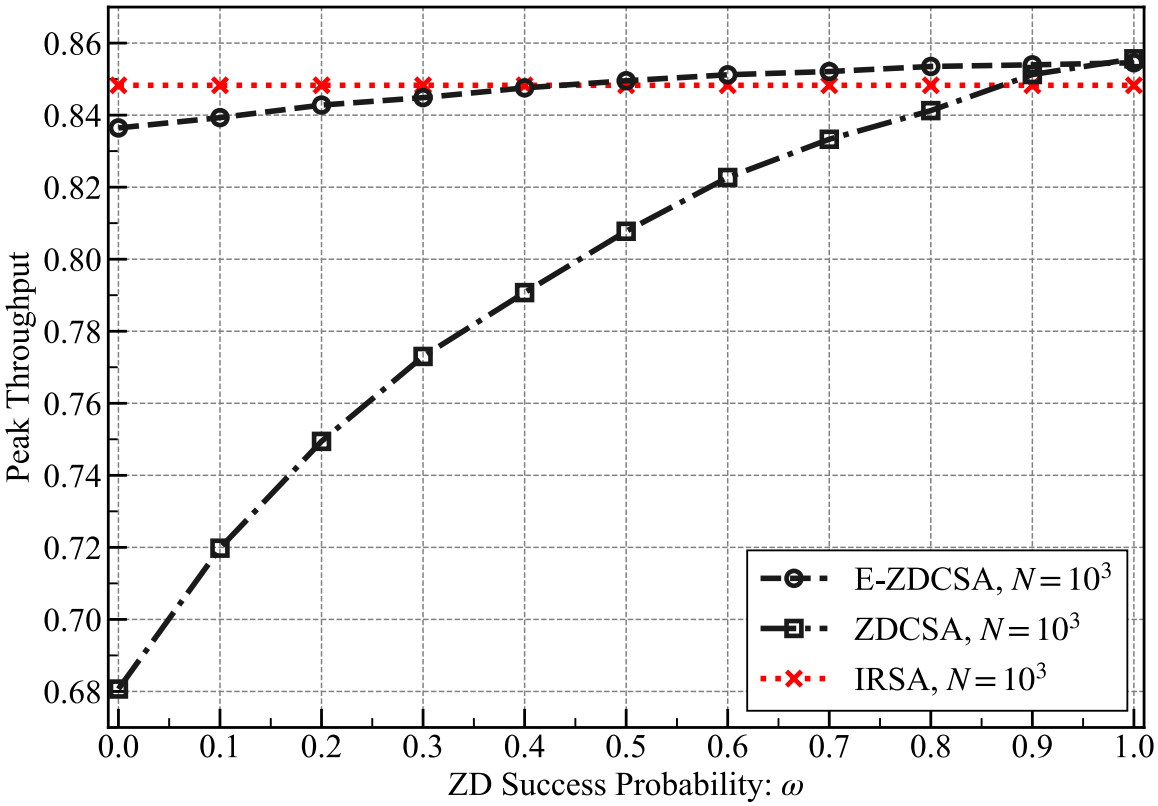

Fig. 6.4 Peak throughput performance with $\omega \in [0,1]$ and $N = 10^3$.

6.2 DIFA

In this section, the performance of our proposed protocols are compared with the conventional coded ALOHA schemes. The settings for this numerical analysis are $R = 500$ [m], $\lambda = 10^{-2}$, $\Gamma_{\text{th}} = 3.75$ [dB], $\sigma^2 = -97.5$ [dBm], and $P_t = 0$ [dBm]. Also, $P(x)$ is set to

$$\begin{aligned} P(x) = {} & 0.062868x^2 + 0.713007x^3 + 0.011527x^4 + 0.013165x^5 \\ & + 0.007012x^6 + 0.009150x^7 + 0.002525x^8 + 0.011213x^9 \\ & + 0.005533x^{10} + 0.015472x^{11} + 0.010295x^{12} + 0.006852x^{13} \\ & + 0.017604x^{14} + 0.008150x^{15} + 0.105627x^{16}, \end{aligned} \tag{6.5}$$

which is derived via differential evolution with $k_{\min} = 2$, $k_{\max} = 16$, $\mu = 0.8$, and $N_{\text{cand}} = 10^2$. Fig. 6.5 shows the improvements of throughput performance via differential evolution.

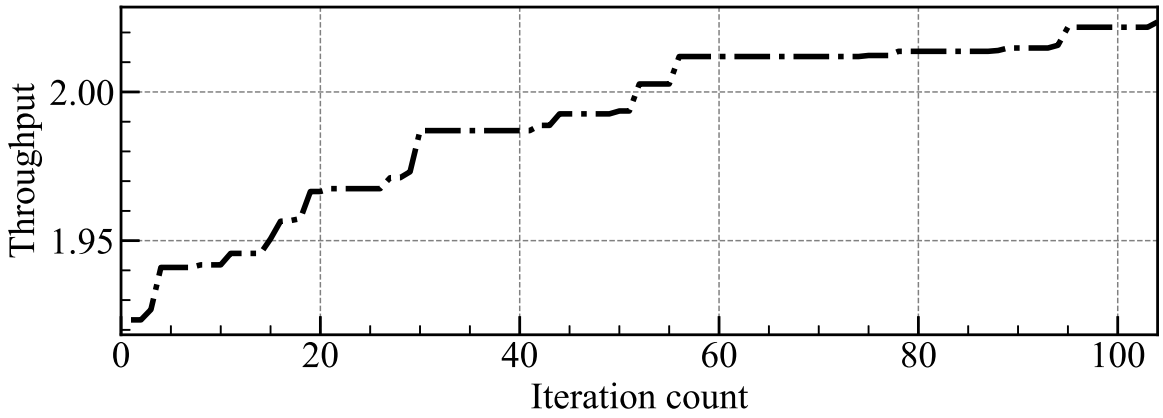

Fig. 6.5 Throughput performance improvement via differential evolution in the case of DIFA

To compare the performance with the conventional scheme [17], we also derived the maximum performance for $L(x) = x^2$.

6.2.1 Throughput and PLR Performances

Fig. 6.6 and Fig. 6.7 show the comparison between each scheme in terms of the throughput and PLR performances, respectively.

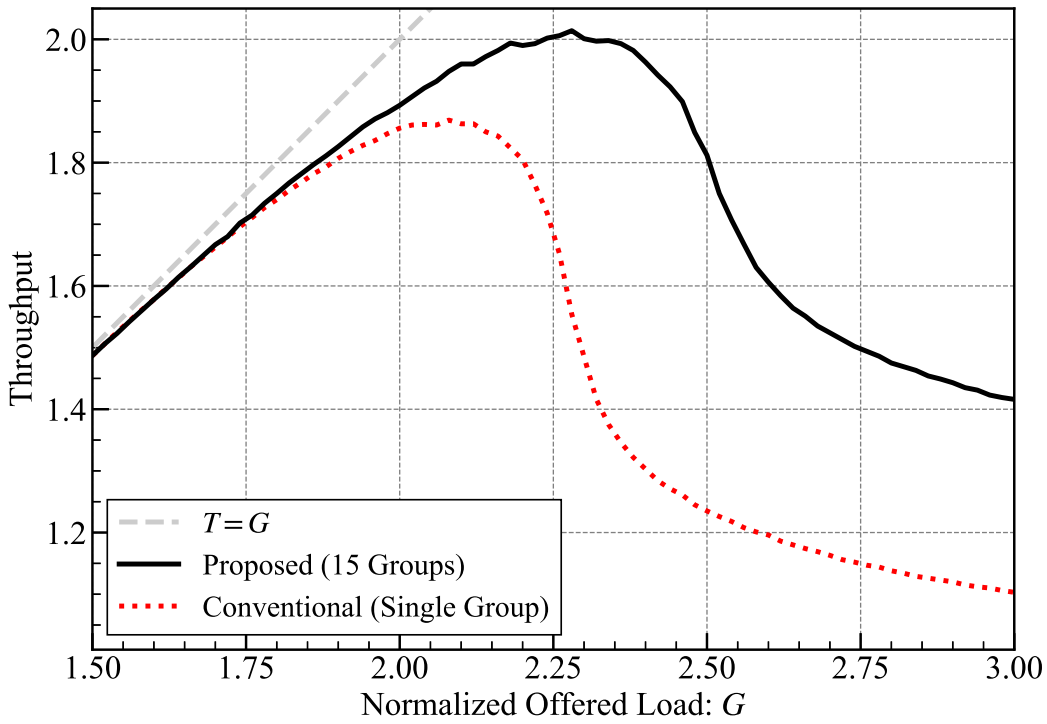

Fig. 6.6 Throughput performances of conventional (single group) and DIFA

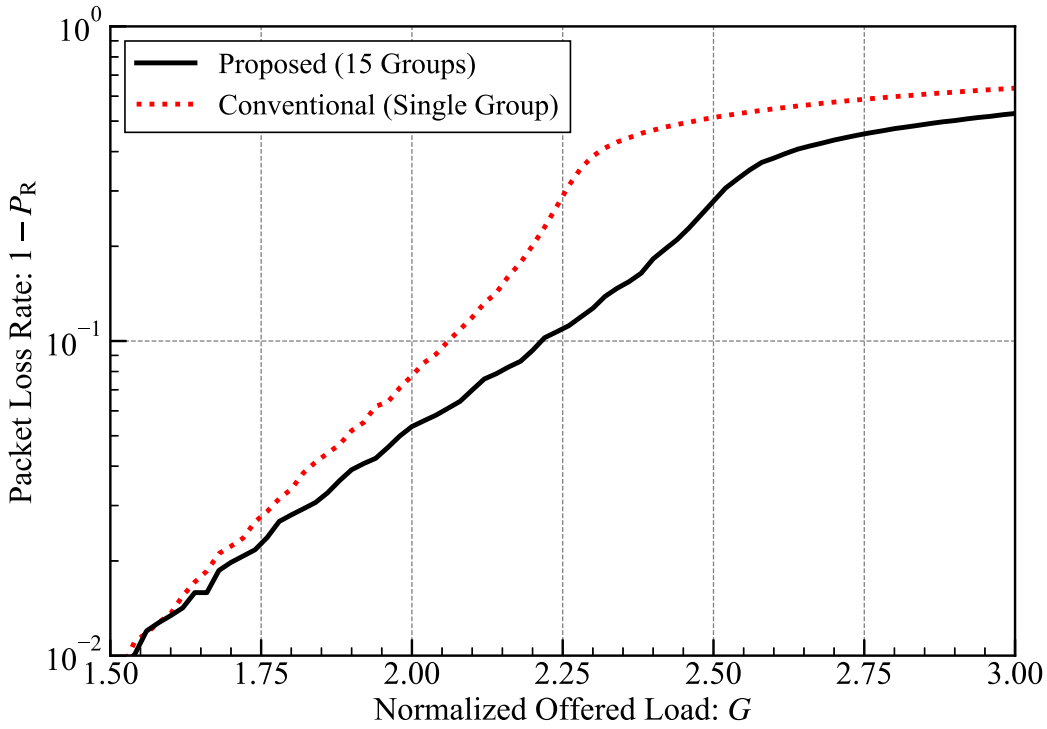

Fig. 6.7 Packet loss rate performances of conventional (single group) and DIFA

From Fig. 6.6 and 6.7, it is shown that our distance-aware design of transmission probability effectively improves the performance of frameless ALOHA with capture effects.

6.2.2 PLR Performance comparison between groups

In order to analyze the proportional fairness between groups, we compare the PLR performance of each group in both conventional frameless ALOHA and proposed DIFA. Note that for frameless ALOHA, the grouping of users is done with probability mass fucntion given in Eq. (6.5) while all users are given the same transmission probability. Also, target degree β and load G is configured to the setting where each protocol achieved the peak throughput performance shown in Fig. 6.6, i.e. $\{\beta, G\} = \{5.9, 2.08\}$ for single group frameless ALOHA and $\{\beta, G\} = \{4.1, 2.30\}$ for DIFA , respectively. Fig. 6.8 shows the result of the PLR of users in the furthest and the closest group, G_2 and G_{16}, for both conventional single group and proposed DIFA.

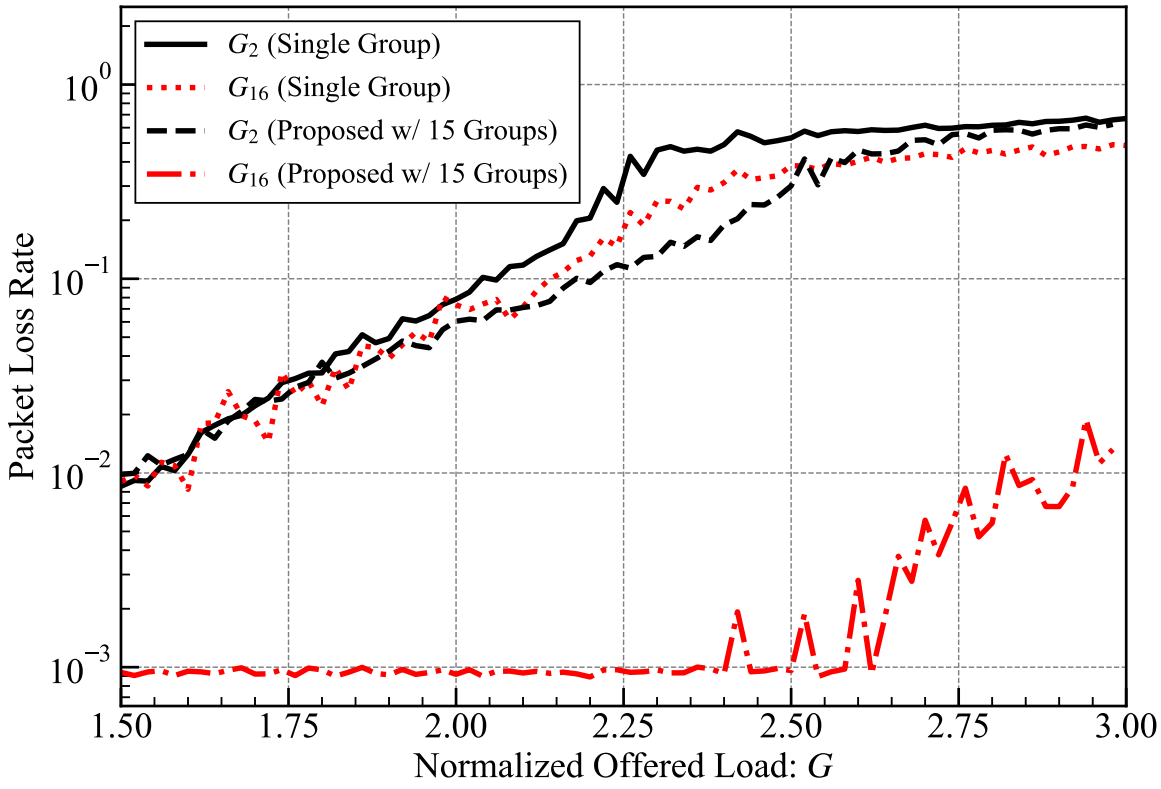

Fig. 6.8 Packet loss rate comparison between G_2, G_{16} of conventional and proposed protocol.

From the Fig. 6.8, the packet loss rate of G_{16} in DIFA with 15 groups is much lower compared to the conventional scheme where the transmission probabilty is shared among all users. Also, the packet loss rate of G_2 in DIFA with 15 groups eventually outperforms the conventional scheme due to the improvement of packet loss rate in G_{16}. Therefore, we can conclude that by utilizing our protocol, not only the closest user but also the furthest user has a benefit in terms of packet loss rate performance.

6.2.3 Degree Distribution of Variable Nodes

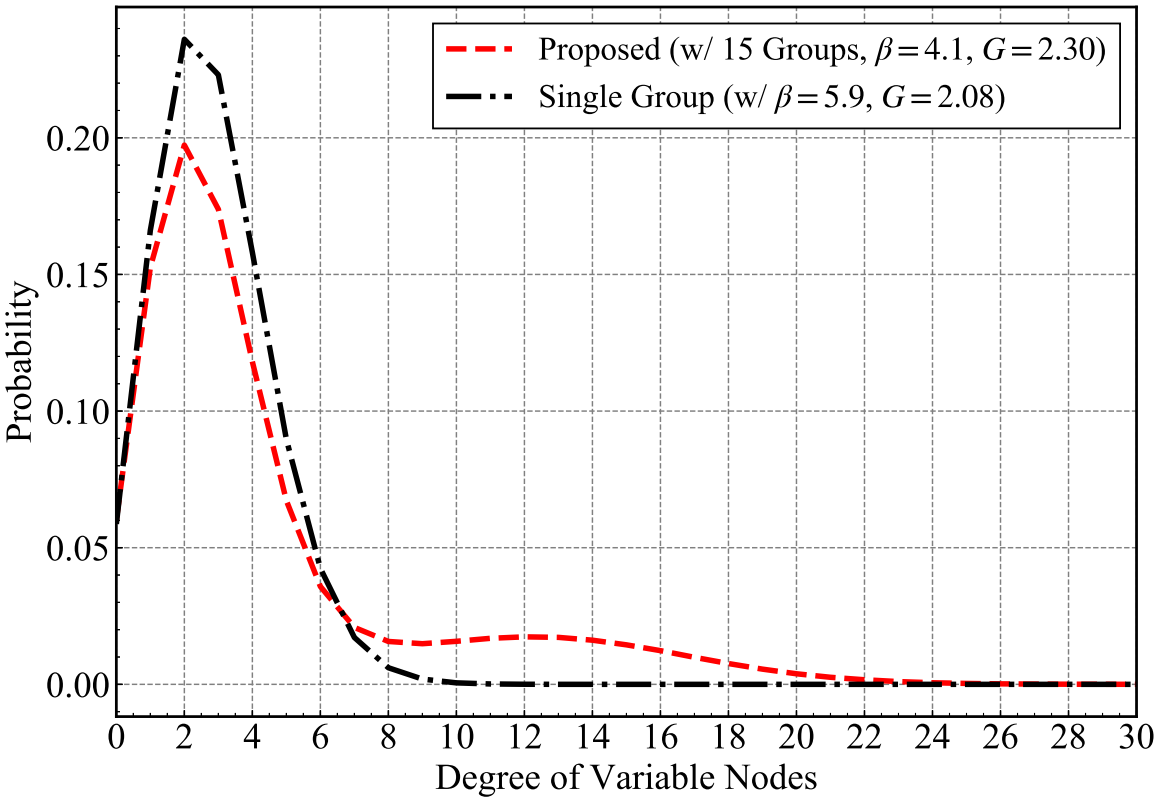

Fig. 6.9 Degree distribution of variable nodes in the conventional and proposed schemes

Finally, we compared the degree distribution of variable node in the case of the conventional (single group) and DIFA (15 groups). In the same manner as previous subsection, the target degree β and load G is configured to the setting where each protocol achieved the peak throughput performance shown in Fig. 6.6, i.e. $\{\beta, G\} = \{5.9, 2.08\}$ for single group frameless ALOHA and $\{\beta, G\} = \{4.1, 2.30\}$ for DIFA , respectively. Fig. 6.9 shows the result of the PLR of users in the furthest and the closest group, G_2 and G_{16}, for both conventional single group and proposed DIFA. As seen from the figure, most of the users in both schemes transmits 2 times within the time frame. Also, since users whose closer to BS transmits more frequently in DIFA, there is a significant increase in the distribution of users whose degree is more than 8 compared to the conventional scheme. Thus leads to not only the improvement in the overall performance, but also the increase of power consumption. Therefore, we have a trade-off when utilizing DIFA where the performance can be improved while the power consumption also increases.

Chapter 7

Conclusion

In this study, the effects of applying ZD into a coded ALOHA scheme in terms of throughput and PLR performances were investigated. Namely, ZDCSA and E-ZDCSA were proposed as a scheme which applies ZD before and after SIC is conducted, respectively. Furthermore, the asymptotic analysis for E-ZDCSA was derived, and its accuracy was validated with the Monte Carlo simulations. Through the numerical and asymptotic analyses, it was revealed that E-ZDCSA outperformed ZDCSA and the conventional IRSA in terms of throughput performance and PLR performance in most of the offered load regime. Moreover, the proposed schemes have also outperformed the conventional scheme in a practical scenario with $\omega \leq 1$. Note that it remains as a future work to take the effects of the physical layer such as capture effects into consideration.

References

[1] G. Liva, "Graph-based analysis and optimization of contention resolution diversity slotted ALOHA," *IEEE Trans. Commun.*, vol. 59, no. 2, pp. 477–487, Feb. 2011.

[2] C. Bockelmann *et al.*, "Towards massive connectivity support for scalable mMTC communications in 5G networks," *IEEE Access*, vol. 6, pp. 28 969–28 992, May 2018.

[3] N. M. Abramson, "The ALOHA system-another alternative for computer communications," *in Proc. 1970 Fall Joint Comput. Conf.*, vol. 37, no. 281–285.

[4] L. G. Roberts, "ALOHA packet system with and without slots and capture," *SIGCOMM Comput. Commun. Rev.*, vol. 5, no. 2, pp. 28–42, Apr. 1975.

[5] E. Casini, R. D. Gaudenzi, and O. del Rio Herrero, "Contention resolution diversity slotted ALOHA (CRDSA): An enhanced random access scheme for satellite access packet networks," *IEEE Trans. Wireless Commun.*, vol. 6, no. 4, pp. 1408–1419, Apr. 2007.

[6] E. Paolini, G. Liva, and M. Chiani, "Coded slotted ALOHA: A graph-based method for uncoordinated multiple access," *IEEE Trans. Inf. Theory*, vol. 61, pp. 6815–6832, Dec. 2015.

[7] T. J. Richardson and R. L. Urbanke, *Modern Coding Theory*. New York, NY, USA: Cambridge University Press, 2008.

[8] R. G. Gallagers, *Low-Density Parity-Check Codes*. Cambridge, MA: M.I.T. Press, 1963.

[9] M. Luby, M. Mitzenmacher, A. Shokrollahi, and D. A. Spielman, "Improved low-density parity-check codes using irregular graphs," *IEEE Trans. Inf. Theory*, vol. 47, no. 2, pp. 585–598, Feb. 2001.

[10] R. Storn and K. Price, "Differential evolution-a simple and efficient heuristic for global optimization over continuous spaces," *J. Global Optim.*, vol. 11, no. 4, pp. 341–359, Dec. 1997.

[11] S. Gollakota and D. Katabi, "Zigzag decoding: Combining hidden terminals in wireless networks," Seattle, WA, USA, Aug. 2008, pp. 159–170.

[12] J. Paek and M. J. Neely, "Mathematical analysis of throughput bounds in random access with ZIGZAG decoding," *in Proc. The 7th Int. ICST Symp. Model. Optim. Mobile, Ad-Hoc, Wireless Netw. (WiOpt)*, pp. 1–7, Jun. 2009.

[13] S. Ogata and K. Ishibashi, "Zigzag decodable frameless ALOHA," in *Proc. The 52nd Asilomar Conf. Signals, Syst., Comput.*, Oct. 2018, pp. 504–507.

[14] ——, "Application of zigzag decoding in frameless ALOHA," *IEEE Access*, vol. 7, pp. 39 528–39 538, 2019.

[15] C. Stefanovic, P. Popovski, and D. Vukobratovic, "Frameless ALOHA protocol for wireless networks," *IEEE Commun. Lett.*, vol. 16, no. 12, pp. 2087–2090, Dec. 2012.

[16] M. Luby, "LT codes," in *Proc. The 43rd Annu. IEEE Symp. Found. Comput. Sci. (FOCS)*, Vancouver, BC, Canada, Nov. 2002, pp. 271–280.

[17] C. Stefanovic, M. Momoda, and P. Popovski, "Exploiting capture effect in frameless ALOHA for massive wireless random access," in *Proc. 2014 IEEE Wireless Commun. Netw. Conf. (WCNC)*, Istanbul, Turkey, Apr. 2014, pp. 1762–1767.

[18] A. Zanella and M. Zorzi, "Theoretical analysis of the capture probability in wireless systems with multiple packet reception capabilities," *IEEE Trans. Commun.*, vol. 60, no. 4, pp. 1058–1071, Apr. 2012.

[19] P. Gupta and P. Kumar, "The capacity of wireless networks," *IEEE Trans. Inf. Theory*, vol. 46, pp. 388–404, Mar. 2000.

[20] M. Haenggi, *Stochastic Geometry for Wireless Networks*. New York, NY, USA: Cambridge University Press, 2012.

[21] H. Kawabata, K. Ishibashi, S. Vuppala, and G. T. F. de Abreau, "Robust relay selection for large-scale energy-harvesting IoT networks," *IEEE Internet Things J.*, vol. 4, no. 2, pp. 384–392, Apr. 2017.

[22] T. J. Richardson, A. Shokrollahi, and R. L. Urbanke, "Design of capacity-approaching irregular low-density parity-check codes," *IEEE Trans. Inf. Theory*, vol. 47, no. 2, pp. 619–637, Feb. 2001.

[23] S. Kullback and R. A. Leibler, "On information and sufficiency," *Ann. Math. Statist.*, vol. 22, no. 1, pp. 79–86, 1951.

[24] A. G. i Amat and G. Liva, "Finite-length analysis of irregular repetition slotted ALOHA in the waterfall region," *IEEE Commun. Lett.*, vol. 22, no. 5, pp. 886–889, May 2018.

Publications

Journal Paper

1. Masaru Oinaga, Shun Ogata, and Koji Ishibashi, "Design of Coded ALOHA with ZigZag Decoder," *IEEE Access*, vol. 7, pp. 168527–168535, Nov. 2019.

International Conference Papers

1. Masaru Oinaga, Shun Ogata, and Koji Ishibashi, "Received-Power-Aware Frameless ALOHA for Grant-Free Non-Orthogonal Multiple Access," in Proc. IEEE 34th Int. Conf. Inf. Netw., pp. 282–285, Barcelona, Spain, Jan. 2020.

2. Masaru Oinaga, Shun Ogata, and Koji Ishibashi, "ZigZag Decoder-Aided Slotted ALOHA with Successive Interference Cancellation," in Proc. IEEE 15th Workshop on Positioning, Navigation and Commun., pp. 1–6, Bremen, Germany, Oct. 2018.

Domestic Conference Papers

1. Masaru Oinaga, and Koji Ishibashi, "Irregular Frameless ALOHA based on Geometric Structure of Devices," IEICE Tech. Rep., vol. 119, no. 436, SeMI2019-124, pp. 65–70, Mar. 2020.

2. Masaru Oinaga, Shun Ogata, and Koji Ishibashi, "On ZigZag-Decoder-Aided Coded Slotted ALOHA," The 42nd Symposium on Information Theory and its Applications (SITA2019), pp. 233–238, Nov. 2019.

3. Masaru Oinaga, Shun Ogata, and Koji Ishiabshi, "Received-Power-Aware Frameless ALOHA for Grant-Free Non-Orthogonal Multiple Access," in Proc. SmartCom 2019 (IEICE Tech. Rep.), vol. 119, no. 262, SR2019-84, pp. 51–51, Rutgers University, NJ, USA, Nov. 2019.

4. Ryo Okabe, Masaru Oinaga, Shun Ogata, and Koji Ishiabshi, "A Study on Energy-Efficient Design of Irregular Repetition Slotted ALOHA with Stochastic Power Control," IEICE Tech. Rep., vol. 119, no. 90, RCS2019-87, pp. 291–296, June 2019.

5. Masaru Oinaga, Shun Ogata, and Koji Ishiabshi, "ZigZag Decodable Coded Slotted ALOHA," IEICE Tech. Rep., vol. 118, no. 101, RCS2018-71, pp. 213–218, June 2018.